Geophysical Research Letters®

Jovian Magnetospheric Injections Observed by the Hubble Space Telescope and Juno

J. D. Nichols[1] , F. Allegrini[2,3] , F. Bagenal[4] , B. Bonfond[5] , G. B. Clark[6] , J. T. Clarke[7] , J. E. P. Connerney[8] , S. W. H. Cowley[1] , R. W. Ebert[2,3] , G. R. Gladstone[2,3] , D. Grodent[5] , D. K. Haggerty[6] , B. Mauk[6] , G. S. Orton[9] , G. Provan[1] , and R. J. Wilson[4]

[1]Department of Physics and Astronomy, University of Leicester, University Road, Leicester, UK, [2]Southwest Research Institute, San Antonio, TX, USA, [3]Department of Physics and Astronomy, University of Texas at San Antonio, San Antonio, TX, USA, [4]Laboratory for Atmospheric and Space Physics, University of Colorado Boulder, Boulder, CO, USA, [5]Laboratory for Planetary and Atmospheric Physics, Université de Liège, Institut d'Astrophysique et de Géophysique—B5c, Liège, Belgium, [6]The Johns Hopkins University Applied Physics Laboratory, Laurel, MD, USA, [7]Center for Space Physics, Boston University, Boston, MA, USA, [8]Goddard Space Flight Center, Greenbelt, MD, USA, [9]Jet Propulsion Laboratory, California Institute of Technology, Pasadena, CA, USA

Abstract We compare Hubble Space Telescope observations of Jupiter's FUV auroras with contemporaneous conjugate Juno in situ observations in the equatorial middle magnetosphere of Jupiter. We show that bright patches on and equatorward of the main emission are associated with hot plasma injections driven by ongoing active magnetospheric convection. During the interval that Juno crossed the magnetic field lines threading the complex of auroral patches, a series of energetic particle injection signatures were observed, and immediately prior, the plasma data exhibited flux tube interchange events indicating ongoing convection. This presents the first direct evidence that auroral morphology previously termed "strong injections" is indeed a manifestation of magnetospheric injections, and that this morphology indicates that Jupiter's magnetosphere is undergoing an interval of active iogenic plasma outflow.

Plain Language Summary Auroras, known as the "Northern (or Southern) Lights" on Earth, are spectacular manifestations of energetic processes occurring in the space environment of a planet. The behavior of Jupiter's magnetosphere is dominated by the planet's rapid rotation, along with the centrifugally-driven outflow of plasma (ionized gas) originating from active volcanoes on the moon Io. A prominent auroral feature on Jupiter has for many years been interpreted as a sign that Jupiter's magnetosphere is undergoing active convection, in which plasma from Io "falls" away from the planet, to be replaced by hot, relatively empty "bubbles" known as injections, moving inward. This feature comprises prominent patches of bright emission that are often observed in Jupiter's auroras, though the evidence associating them with injections has been largely circumstantial. Here we show that the NASA Juno spacecraft flew through such injections in the equatorial magnetosphere on magnetic field lines mapping to a cluster of auroral patches as observed by HST. The Juno data also indicated the interval was characterized by signatures of convection and outflow of plasma originating from Io. This demonstrates that auroral patches are signatures of injections, and that auroral emissions are an important tool for diagnosing the behavior of planetary magnetospheres.

1. Introduction

The dynamics of Jupiter's magnetosphere are dominated by rotation and centrifugal outflow of plasma originating from the moon Io. The process by which this outflow occurs is not well understood, but a principal mechanism is thought to be flux tube interchange, in which magnetic flux tubes loaded with cold plasma interchange radially with flux tubes populated by less dense, hot plasma moving inward (e.g., Kivelson et al., 1997). These inward injections of energetic particles have been observed by Galileo (Mauk et al., 1999, 2002) and more recently by Juno (Haggerty et al., 2019), and comprise transient intervals of elevated particle energies and a characteristic energy dispersion signature. Plasma injections have been implicated as the cause of corotating, bright patches of far-ultraviolet (FUV) aurora that often appear in clusters on or equatorward of the main auroral emission on Jupiter (e.g., Dumont et al., 2018), to the extent that Grodent et al. (2018) named auroral morphology families exhibiting these features "injections," and they are often named as such in the literature. The association is strengthened by the observation that the statistics of their location when mapped to the equatorial magnetosphere

are consistent with those of observed injections (Dumont et al., 2014). The dynamics of adjacent auroral forms have been taken as evidence relating auoral patches with radial transport of plasma (Gray et al., 2016), and they have been observed to appear following dawn storms, which are thought to be associated with large-scale night-side dipolarization (Bonfond et al., 2021; Ebert et al., 2021; Swithenbank-Harris et al., 2021; Yao et al., 2020). Spectral scans by the Juno ultraviolet spectrometer (UVS (Gladstone et al., 2017)) and Space Telescope Imaging Spectrograph (STIS) onboard the Hubble Space Telescope (HST) show gradients in the color ratio across patches indicative of energy dispersion characteristic of injections (Dumont et al., 2018; Haggerty et al., 2019). Patches reported by J. D. Nichols, Badman, et al. (2017) were observed ∼10 days following a sodium nebula enhancement, possibly indicating enhanced volcanic activity (Morgenthaler et al., 2019), but were also coincident with a solar wind rarefaction, the occurrence of which has been linked to clusters of injections (Mauk et al., 1999). Two possible mechanisms for production of aurora are: (a) precipitation of energetic electrons within the injections, with the loss cone replenished by pitch angle scattering due to wave-particle interactions, or (b) continuity currents that flow at the leading and poleward edges of localized enhanced ring current associated with the hot plasma, with the upward component residing at the trailing edge at Jupiter, as at Saturn (Mauk et al., 2002; J. D. Nichols et al., 2014).

Overall, the observational association of auroral patches with plasma injections and magnetospheric convection is largely based on the circumstantial evidence outlined above. Only one injection has been observed in situ in the equatorial magnetosphere contemporaneously with an isolated low latitude auroral patch observed by HST (Mauk et al., 2002). Those authors reported injections observed by Galileo over a ∼5 hr interval on 28 December 2000, during which the spacecraft trajectory, when mapped along the magnetic field to the ionosphere, passed through the patch for around ∼30 min. The HST image was obtained ∼2.5 hr prior to Galileo's intersection with the patch. This remained the only example of dual particle and remote sensing observations of patches and injections until Haggerty et al. (2019) reported observations from the vantage point of the high latitude magnetosphere, when Juno was near to perijove (PJ). They reported injections observed during a number of PJ passes, and focused on one set (PJ8) with UVS observations of patches. Multiple patches were observed, along with a ∼4 hr interval of injection signatures, but again, only a single auroral patch was magnetically conjugate with an injection. They concluded that the relationship between auroral patches and injections was more complicated than expected. To date, therefore, there have been no observations of "injection" auroral patch clusters while a spacecraft is in the conjugate equatorial magnetosphere, providing a full complement of in situ observations, such that the relation between auroral patches, injections, and flux tube interchange remains tenuous.

Here, we report HST observations of Jupiter's FUV auroras, along with simultaneous Juno in situ observations while the spacecraft was in the equatorial middle magnetosphere. We show that a complex of multiple auroral patches observed by HST was magnetically conjugate with an interval of magnetospheric injection signatures observed by Juno, and that the magnetosphere was at the time undergoing active flux tube interchange, indicating an episode of ongoing magnetospheric convection and mass outflow. This provides the first direct evidence of the association between auroral patches and magnetospheric convection conjectured previously (e.g., Bonfond et al., 2021; Dumont et al., 2014; Grodent et al., 2018), and demonstrates that auroral morphology is an important diagnostic of the state of mass outflow activity at Jupiter.

2. Data

The auroral data were obtained using STIS onboard HST as part of program GO-16989. Jupiter's FUV auroras were observed using the F25SRF2 filter, which admits light in the H_2 Lyman and Werner bands. Observations were obtained in 1-orbit visits, and those considered here are visits 06 and 07. Images with integration times of 30 s were extracted and reduced using the University of Leicester implementation of the Boston University pipeline, which has been used extensively in previous studies (e.g., Clarke et al., 2009; J. D. Nichols, Yeoman, et al., 2017; J. D. Nichols et al., 2009, 2020). The Juno data employed are from the Juno Magnetic Field Investigation (MAG) (Connerney et al., 2017), Jupiter Energetic Particle Detector Instrument (JEDI) (Mauk et al., 2017), and the Jovian Auroral Distributions Experiment (JADE) (McComas et al., 2017) instruments. The MAG data used are the 60 s planetocentric data transformed to magnetic cylindrical polar coordinates (ρ, ϕ, z) with z aligned with the JRM33 dipole axis (Connerney et al., 2022). A Figure showing Juno's trajectory during this interval is shown in Supporting Information S1. The local time of the spacecraft was ∼19 hr LT, and Juno was mainly in the southern middle magnetosphere, moving inward at radial distances of ∼15 R_J (1 R_J = 71, 492 km). Throughout

each planetary rotation, Juno swept through z owing to the tilt of the planet's magnetic dipole. During the interval of the HST observations, Juno was moving in toward the magnetic equator from $z \sim -5$ R$_J$, crossing the Ganymede flux shell and the magnetic equator $\sim$1 hr later.

3. Analysis

Representative images from each HST visit are shown in Figure 1; Movies S1 and S2. Both visits exhibit broken and disordered main emission (ME) characterized by arcs and patches, the latter extending to lower latitudes, along with relatively bright equatorward diffuse emission. The intensity peaks at $\sim$12 MR in the large patch labeled A extending from $\sim$153–178° System III(1965) longitude (λ_{III}) and $\sim$2.8 MR in the form situated at $\lambda_{III} \sim$ 165–170°, labeled B. A further form at $\lambda_{III} \sim$ 162° is labeled C. The wider diffuse equatorward emission was typically a few hundred kR. This overall morphology corresponds to Family I ("Strong Injections") defined by Grodent et al. (2018), the name reflecting a "likely" association with magnetospheric plasma injections. Over the two visits, patch A broke up into several smaller corotating spots. Patches B and C also stayed essentially fixed in λ_{III}. A plot of the intensity in patch B determined from the mean of the emission contained within the corotating red box drawn in Figure 1, is shown in Figure 2b. The patch dimmed from $\sim$2.8 MR to $\sim$1.1 MR over the course of the two visits. The yellow and green regions plotted over the projections show the Juno spacecraft trajectory mapped by field-line tracing using the JRM33 internal field (Connerney et al., 2022) and magnetodisc (Connerney et al., 1981) models. The uncertainty in mapping due to variable azimuthal current and radial stretching of the field is shown by the width of the yellow line, illustrating results using the range azimuthal current intensities calculated by Connerney et al. (2020), that is, $\mu_0 I_0 = 242$–561 nT. It is evident that the spacecraft directly traversed the field lines threading patches B and C $\sim$1–2.5 hr following the end of visit 07, and grazed the equatorward edge of patch A $\sim$1 hr later.

We illustrate this further with keograms in Figure 2a, computed with the spatial coordinate given by the spacecraft mapped trajectory. See the SI for further details but, briefly, for each extracted image, we have obtained the mean of the auroral intensity over 5×5 pixel boxes centered on each mapped trajectory coordinate, computed with 25 s resolution, which yields the horizontal axis in Figure 2a. We have considered the time interval between the start of visit 06 at 0945 hr and 1500 hr, indicated by the green portion of the spacecraft trajectory in Figure 1. The 1D intensity profiles obtained from each image are then stacked to give the vertical axis in Figure 2a, with the coordinate being the starting time of each 30 s exposure. The diagonal black line with negative unit slope then corresponds to the track of Juno as it moves along the mapped trajectory. Clearly, only the two intervals corresponding to the times of the HST exposures, where the Juno track intersects the keograms, provide a true reflection of the auroral morphology at the footprint of the in situ observations, and other times require extrapolation of the auroral morphology, for which care must be taken. Nevertheless, it is reasonable to suppose that the patch A and the complex including patches B, and C (labeled in the keogram) remained fixed over the interval, even if the intensity varied as for for example, patch B in Figure 2b. Two empirical methods of estimating the intensity of patch B at the time of intersection at $\sim$1400 hr are shown, assuming either exponential decay fitted to both visits or a linear fit to the second visit. Both yield intensities of $\sim$300–500 kR. Of course, the brightness may have instead remained around $\sim$1 MR or the morphology may have changed completely. Given the broad similarities between the morphologies in visits 06 and 07, separated by $\sim$1.5 hr, we consider the latter unlikely. However, in light of this uncertainty, we have limited the extrapolation to 3 hr following visit 07. Clearly this is somewhat arbitrary, but seems reasonable given the evident timescale of the variation of auroral intensity.

With this caveat in mind, we turn now to the Juno MAG, JEDI electron and JADE proton data shown in Figure 3. Starting with the magnetic field shown in Figures 3a–3c, at the time of the HST observations shown by the gray vertical bars, the spacecraft resides near the edge of the azimuthal current sheet, entering the sheet and crossing the center around $\sim$1300 hr according to the B_ρ data, in accordance with expectation based on the trajectory in Figure 3f. During this interval, the spacecraft remains equatorward of the magnetosphere-ionosphere field-aligned current sheet and associated lagging B_φ field briefly evident before the HST exposures, such that the azimuthal field takes low values. The lagging B_φ itself is significant, peaking at $\sim$17 nT, that is, a factor of $\sim$2 larger than expectation based on the Leicester magnetosphere-ionosphere coupling (L-MIC) model (Cowley et al., 2017). The data are noisy, indicative of the presence of hot plasma, and there is no evidence that the spacecraft re-emerges from the radial current sheet. Overall, the magnetic field data reveal the occurrence of magnetosphere-ionosphere coupling associated with significant ongoing mass outflow but, given the equatorial
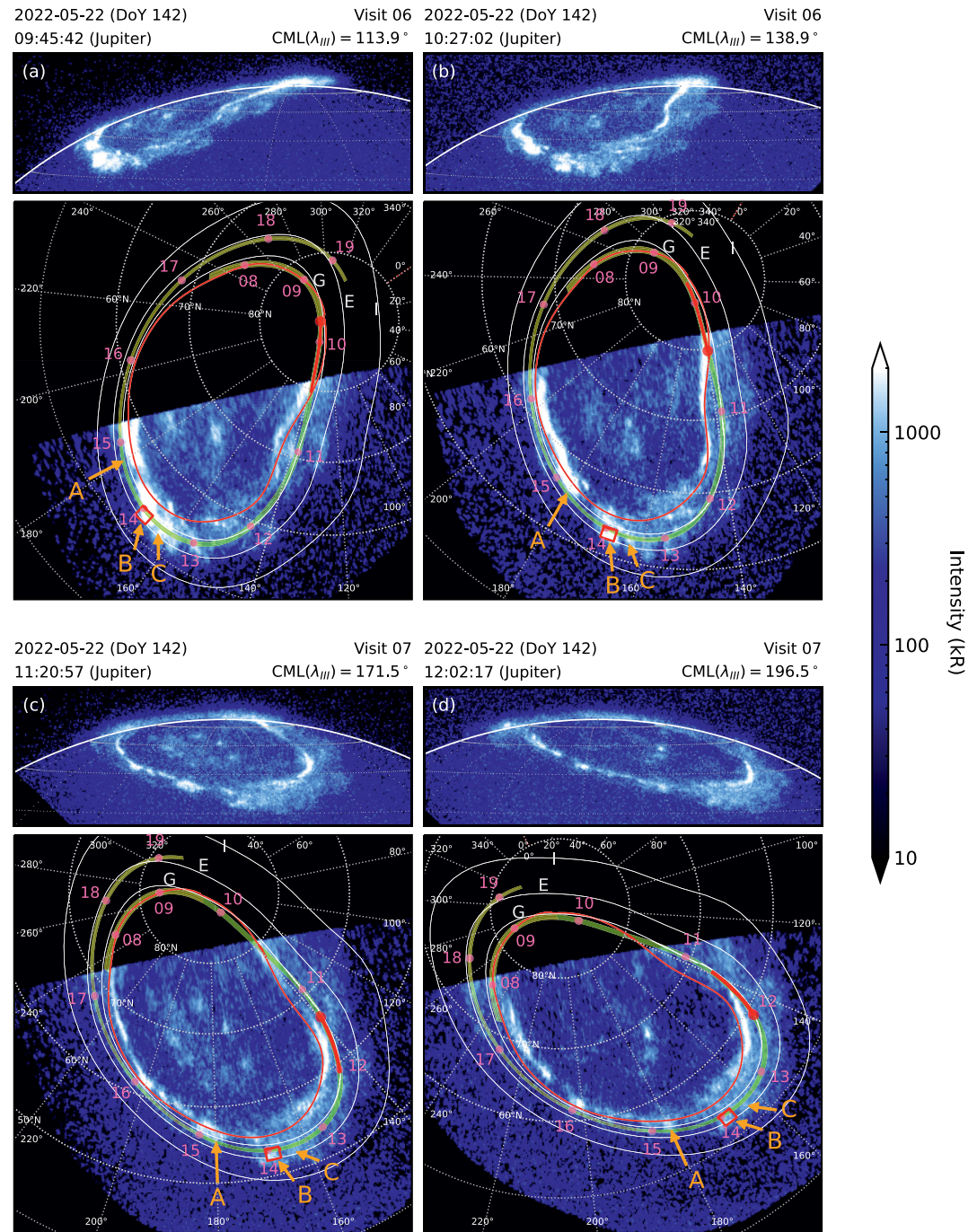
Figure 1. Images from the start and end of each visit. Exposure times (corrected for light travel time) and central meridian longitude (CML) are labeled. In each panel (a–d) we show the unprojected images above and projected images below, presented in a polar stereographic projection from above the north. The sub-solar longitude is toward the bottom, dawn to the left and dusk to the right. Yellow and green regions denote the mapped Juno trajectory as described in the text, while the red line shows the portion of the mapped trajectory covered during the Hubble Space Telescope exposure. Red circles indicated the mapped location of Juno during the particular image shown. Hour markers are shown in magenta. The red box denotes the intensity extraction region discussed in the text. Solid gray lines show the mapped Galilean satellites contours, while the closed red line shows the J. D. Nichols, Badman, et al. ([2017](#)) reference main oval. A $10° \times 20°$ graticule is shown with labeled dotted gray lines. Particular auroral patches discussed in the text are labeled A–C. Auroral intensity is shown on a log scale as indicated by the color bar.
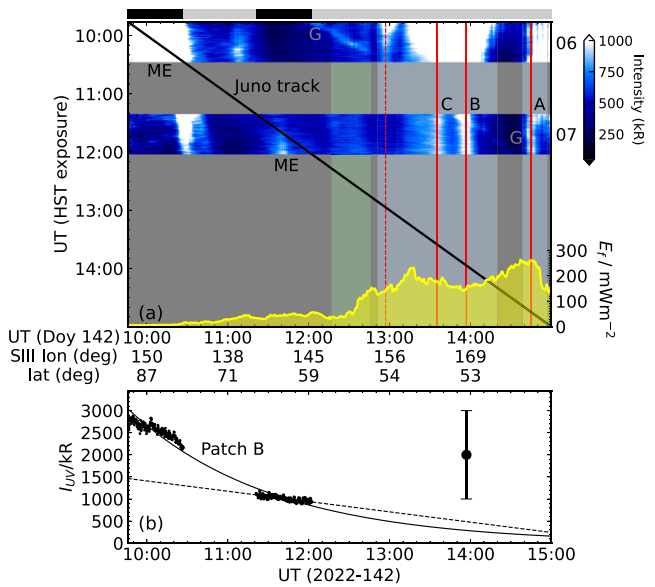
Figure 2. Plot showing (a) keograms of auroral intensity computed along the spacecraft trajectory as discussed in the text, and (b) the evolution of intensity of patch B. In panel (a), the horizontal axis is the timestamp of the mapped Juno trajectory. The auroral features labeled are the main emission (ME), the Ganymede footprint (G) and auroral patches A, B, and C. The black solid line shows the mapped Juno track. The times of the Hubble Space Telescope exposures are highlighted in the horizontal axis by the black bars at the top, the gray bars representing other times. Vertical red lines indicate the particular auroral patches, and the shaded vertical bars indicate the locations of wider patch complexes and features. The yellow plot shows the JEDI energetic particle field-aligned energy fluxes. In panel (b) the solid and dashed lines show estimates of the intensity of Patch B assuming a linear fits to $\ln(I_{UV})$ including both visits (solid line) and to I_{UV} including only visit 07 (dashed line). The point with the error bar illustrates the range of auroral intensities implied by the energy fluxes in the injection interval.

location of the spacecraft following the HST observations, there is no evidence of large current signatures later in the interval, rather only an indication of the presence of hot plasma.

Turning now to the energetic electron data shown in Figure 3d (and discussed further in the SI), the principal feature of interest is the presence of multiple magnetospheric injection signatures after ~1230 hr UT. These signatures are bursts of elevated electron energies up to a few hundred keV. They exhibit characteristic energy dispersion related to the time since formation, and estimation of their age using the method of Haggerty et al. (2019) yields ~1.5 ± 0.5 hr, implying the injection process finished around the time of visit 07. Also shown is the electron kinetic energy flux contained within 20° of the anti-magnetic field direction, as close to the loss cone as JEDI can resolve. In the sequence of injections between ~1230 hr and ~1500 hr, the energy fluxes are around ~100–300 mW m⁻², which if precipitated into the ionosphere and assuming the canonical conversion efficiency (Gérard & Singh, 1982; Grodent et al., 2001; J. D. Nichols & Cowley, 2022; Waite et al., 1983) would yield FUV auroral intensities of ~1–3 MR, consistent with the 1.1–2.8 MR observed in patch B (Figure 2b). This implies that either the auroral intensities did not continue to fade after visit 07, or the precipitating energy flux was actually somewhat lower than estimated here. The implication is at least that the energetic electrons detected are easily capable of producing the FUV aurora observed. We have also plotted the anti-field-aligned energetic electron energy flux in the keogram in Figure 2a. It is evident that the broad interval of enhanced energy fluxes is consistent with the location of the complex of auroral patches, as shown by the light blue rectangles. It is less straightforward to identify individual auroral patches with particular injection signatures, likely because of the time gap between the HST and injection observations. Patch A can plausibly be linked to the peak in energy flux at 1445 hr. Patch B is coincident with a minimum in energy fluxes, while patch C may be associated with the lesser peaked region around 1315 hr. There is a fainter auroral feature highlighted by the green rectangle (note, drawn behind the keograms) that perhaps corresponds to the leading edge of the interval of enhanced energy fluxes, but this is not a strong association. A further feature

present in visit 06 but not in visit 07 is highlighted by the dashed line also lies within the interval of enhanced energy fluxes. It is finally worth noting that the ~50 mW m⁻² energy fluxes observed between ~1100 hr and the onset of the injections are consistent with the ~500 kR equatorward diffuse emission observed along and around the Juno trajectory. Considering now the JADE proton energy spectra shown in Figure 3e, the principal features of interest are signatures of flux tube interchange events in the interval from ~0730 hr to ~1100 hr, consisting of alternating intervals of cold (few hundred eV) and hotter (1–10 keV) plasma. Flux tube interchange is indicative of ongoing magnetospheric convection, which is consistent with the production of inward injections of hot plasma, if not necessarily causally related to those observed here. The magnetosphere is more densely populated with plasma than during intervals when the auroral morphology is less disturbed, as indicated in Figure 4, which shows a comparison with HST and JADE heavy ion data obtained on 16 October 2021, when Juno was in an essentially identical meridional location. On 22 May the number density was overall higher and more variable.

4. Discussion

Overall, these results demonstrate that auroral clusters of bright patches accompanied by bright equatorward diffuse emission are associated with hot plasma injections and ongoing active magnetospheric convection and outflow of iogenic plasma. The series of injections observed by JEDI was magnetically conjugate with the complex of auroral patches observed around an hour previously by HST. It is not straightforward to associate individual patches with particular injection signatures, though this is perhaps unsurprising. Our analysis relies on the auroral morphology not changing dramatically between HST observation and the spacecraft's track crossing the patches, though as noted above this does not seem likely, given the timescale of changes in the auroral forms.
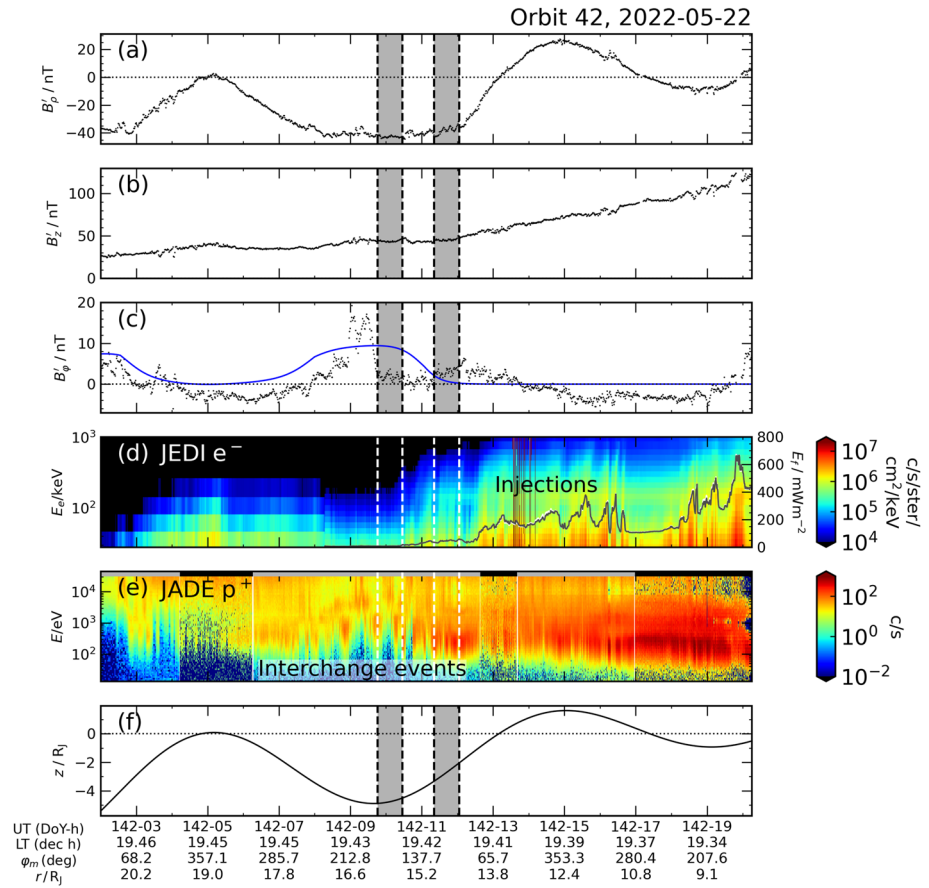
Figure 3. Juno in situ data obtained during this interval. The top three panels (a–c) show magnetic field components after subtraction of the JRM33 internal planetary field B'_ρ, B'_z and B'_φ in nT in magnetic coordinates. The blue line in panel (c) show the L-MIC model values. Panel (d) shows the JEDI electron energy spectra along with the anti-field-aligned energy flux in mW m⁻². Panel (e) shows the Jovian Auroral Distributions Experiment proton energy spectra, and panel (f) shows Juno's z position relative to the Khurana and Schwarzl (2005) current sheet center. The gray regions bound by the dashed lines illustrate the Hubble Space Telescope exposure times, corrected for light travel. In panel (e) the gray and black bars at the top indicate intervals of low resolution and high resolution data, respectively.

We also note that the Mauk et al. (2002) event was observed by HST ~2.5 hr before being crossed by Galileo. Perhaps more likely is steady evolution of the morphology, for example, patches could fade or move. Dumont et al. (2018) showed that such patches tend to modestly subrotate (>80% of rigid corotation) and drift equatorward by up to 1° h⁻¹. This would modify the auroral intensity along the spacecraft track from that suggested by the keograms, and this may explain the lack of obvious association between small-scale variations in auroral intensity and the particle energy flux. Two obvious discrepancies are that patch B apparently corresponds to a minimum in energy flux, and the interval between ~1400 and ~1440 hr corresponds to relatively low auroral intensities, despite the field-aligned energy flux being close to their maximum. Similar discrepancies were noted in the high latitude observations of Haggerty et al. (2019). An explanation for patch B could be that, as noted above, regions of hot plasma are expected to be bound on the leading and trailing edges by field-aligned currents, with the upward component residing on the trailing edge. This could be the cause of patch B, though this cannot be confirmed by the MAG data, since Juno was very close to the current sheet center. The dark region between ~1400 and ~1440 hr is less easy to explain, except via auroral morphology variation. Further, while we have limited the detailed analysis to before 1500 hr, it is evident that the first series of injections continued until ~1700 hr, and indeed auroral patches are observed around to $\lambda_{III} \sim 240°$, which Juno's mapped trajectory crossed at ~1720 hr. These patches are poleward of the mapped spacecraft trajectory, but equatorward motion at the rates reported by Dumont et al. (2018) could easily lead to patches overlapping Juno's trajectory by ~1700 hr. Indeed, the equatorward boundary of patch B moved equatorward by ~1° over the interval.
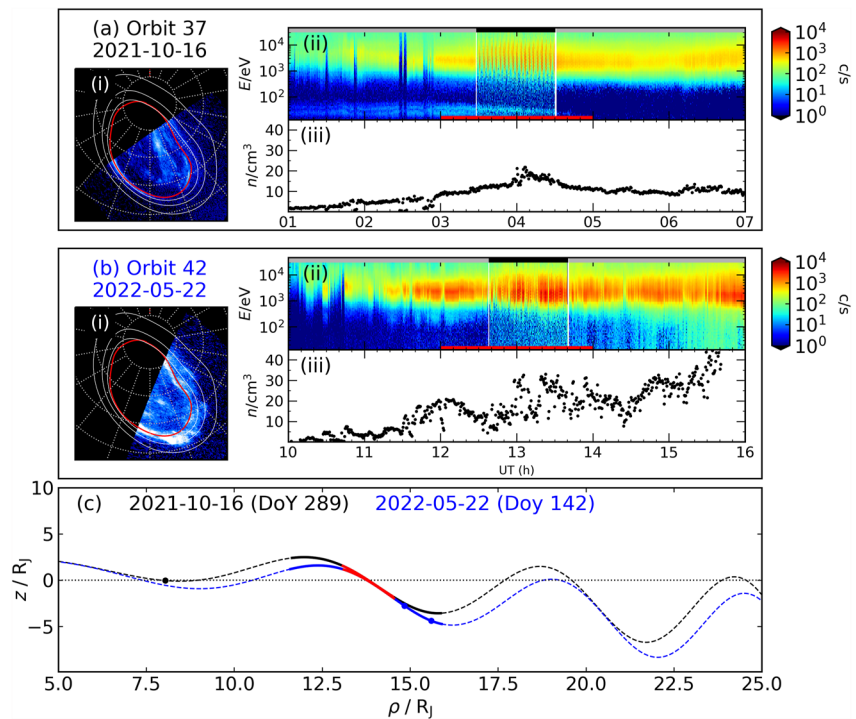
Figure 4. Comparison between the Hubble Space Telescope and Jovian Auroral Distributions Experiment (JADE) heavy ion data obtained on (a) 16 Oct 2021 and (b) 22 May 2022. In panels (a, b) we show (i) projected images with SIII longitude 180° toward the bottom, (ii) JADE heavy ion data in the same format as Figure 3e, except that the red bars at the bottom of each panel indicate the times corresponding to the trajectory in panel (c) shown in red, and (iii) heavy ion number density in cm^{-3}. The z position of the spacecraft is shown in panel (c), with the black and blue colors denoting the epochs as labeled. The red sections indicate when the meridional coordinates are similar for the two epochs. The thick solid sections of the trajectory lines indicate the interval for which data are plotted in panels (a, b).

5. Summary

We have compared HST observations of Jupiter's FUV auroras with contemporaneous Juno in situ observations in the equatorial middle magnetosphere of Jupiter, and shown that:

- Bright patches and bright equatorward diffuse emission are associated with hot plasma injections driven by ongoing active magnetospheric convection.
- HST observed a cluster of bright patches that was magnetically conjugate with a series of energetic particle injections observed by Juno.
- The plasma data exhibited flux tube interchange events indicating ongoing convection and the magnetometer revealed enhanced magnetosphere-ionosphere coupling.
- The heavy ion density was higher and more variable than a comparable interval when no patches and diffuse emission were observed.

This presents the first direct evidence that auroral morphology previously termed "strong injections" is indeed a manifestation of magnetospheric injections, and that this indicates that Jupiter's magnetosphere is undergoing an interval of active iogenic plasma outflow.

Data Availability Statement

The HST data are available at MAST (J. D. Nichols, 2023). Juno data are from the MAG (Connerney, 2022), JADE (Allegrini et al., 2022) and JEDI (Mauk, 2022) datasets available at the NASA PDS.

References

Allegrini, F., Wilson, R. J., Ebert, R. W., & Loeffler, C. (2022). Juno J/SW Jovian auroral distribution calibrated V1.0, JNO-J/SW-JAD-3-calibrated-V1.0 [Dataset]. NASA Planetary Data System. https://doi.org/10.17189/1519715

Bonfond, B., Yao, Z. H., Gladstone, G. R., Grodent, D., Gérard, J.-C., Matar, J., et al. (2021). Are dawn storms Jupiter's auroral substorms? *AGU Advances*, *2*(1), e2020AV000275. https://doi.org/10.1029/2020AV000275

Clarke, J. T., Nichols, J. D., Gérard, J.-C., Grodent, D., Hansen, K. C., Kurth, W. S., et al. (2009). Response of Jupiter's and Saturn's auroral activity to the solar wind. *Journal of Geophysical Research*, *114*(A), A05210. https://doi.org/10.1029/2008ja013694

Connerney, J. E. P. (2022). Juno MAG calibrated data J V1.0, JNO-J-3-FGM-CAL-V1.0 [Dataset]. NASA Planetary Data System. https://doi.org/10.17189/1519711

Connerney, J. E. P., Acuña, M. H., & Ness, N. F. (1981). Modeling the Jovian current sheet and inner magnetosphere. *Journal of Geophysical Research*, *86*(A10), 8370–8384. https://doi.org/10.1029/ja086ia10p08370

Connerney, J. E. P., Benn, M., Bjarno, J. B., Denver, T., Espley, J., Jorgensen, J. L., et al. (2017). The Juno magnetic field investigation. *Space Science Reviews*, *73*(11), 1–100. https://doi.org/10.1007/s11214-017-0334-z

Connerney, J. E. P., Timmins, S., Herceg, M., & Joergensen, J. L. (2020). A Jovian magnetodisc model for the Juno Era. *Journal of Geophysical Research: Space Physics*, *125*(10), e2020JA028138. https://doi.org/10.1029/2020JA028138

Connerney, J. E. P., Timmins, S., Oliversen, R. J., Espley, J. R., Joergensen, J. L., Kotsiaros, S., et al. (2022). A new model of Jupiter's magnetic field at the completion of Juno's prime mission. *Journal of Geophysical Research: Planets*, *127*(2), e2021JE007055. https://doi.org/10.1029/2021JE007055

Cowley, S., Provan, G., Bunce, E., & Nichols, J. (2017). Magnetosphere-ionosphere coupling at Jupiter: Expectations for Juno Perijove 1 from a steady state axisymmetric physical model. *Geophysical Research Letters*, *44*(10), 4497–4505. https://doi.org/10.1002/2017GL073129

Dumont, M., Grodent, D., Radioti, A., Bonfond, B., & Gérard, J.-C. (2014). Jupiter's equatorward auroral features: Possible signatures of magnetospheric injections. *Journal of Geophysical Research: Space Physics*, *119*(12), 10068–10077. https://doi.org/10.1002/2014JA020527

Dumont, M., Grodent, D., Radioti, A., Bonfond, B., Roussos, E., & Paranicas, C. (2018). Evolution of the auroral signatures of Jupiter's magnetospheric injections. *Journal of Geophysical Research: Space Physics*, *123*(10), 8489–8501. https://doi.org/10.1029/2018JA025708

Ebert, R. W., Greathouse, T. K., Clark, G., Hue, V., Allegrini, F., Bagenal, F., et al. (2021). Simultaneous UV images and high-latitude particle and field measurements during an auroral dawn storm at Jupiter. *Journal of Geophysical Research: Space Physics*, *126*(12), e2021JA029679. https://doi.org/10.1029/2021JA029679

Gérard, J. C., & Singh, V. (1982). A model of energy deposition of energetic electrons and EUV emission in the Jovian and Saturnian atmospheres and implications. *Journal of Geophysical Research*, *87*(A6), 4525–4532. https://doi.org/10.1029/ja087ia06p04525

Gladstone, G. R., Persyn, S. C., Eterno, J. S., Walther, B. C., Slater, D. C., Davis, M. W., et al. (2017). The ultraviolet spectrograph on NASA's Juno Mission. *Space Science Reviews*, *213*(1), 447–473. https://doi.org/10.1007/s11214-014-0040-z

Gray, R. L., Badman, S. V., Bonfond, B., Kimura, H., Misawa, H., Nichols, J. D., et al. (2016). Auroral evidence of radial transport at Jupiter during January 2014. *Journal of Geophysical Research: Space Physics*, *121*(10), 9972–9984. https://doi.org/10.1002/2016JA023007

Grodent, D., Bonfond, B., Yao, Z., Gérard, J.-C., Radioti, A., Dumont, M., et al. (2018). Jupiter's aurora observed with HST during Juno Orbits 3 to 7. *Journal of Geophysical Research: Space Physics*, *123*(5), 3299–3319. https://doi.org/10.1002/2017JA025046

Grodent, D., Waite, J. H., & Gérard, J.-C. (2001). A self-consistent model of the Jovian auroral thermal structure. *Journal of Geophysical Research*, *106*(A7), 12933–12952. https://doi.org/10.1029/2000JA900129

Haggerty, D. K., Mauk, B. H., Paranicas, C. P., Clark, G., Kollmann, P., Rymer, A. M., et al. (2019). Jovian injections observed at high latitude. *Geophysical Research Letters*, *46*(16), 9397–9404. https://doi.org/10.1029/2019GL083442

Khurana, K. K., & Schwarzl, H. K. (2005). Global structure of Jupiter's magnetospheric current sheet. *Journal of Geophysical Research*, *110*(A7), 8385.

Kivelson, M. G., Khurana, K. K., Russell, C. T., & Walker, R. J. (1997). Intermittent short-duration magnetic field anomalies in the Io torus: Evidence for plasma interchange? *Geophysical Research Letters*, *24*(17), 2127–2130. https://doi.org/10.1029/97gl02202

Mauk, B. H. (2022). JEDI calibrated (CDR) data JNO J JED 3 CDR V1.0 [Dataset]. NASA Planetary Data System. https://doi.org/10.17189/1519713

Mauk, B. H., Clarke, J. T., Grodent, D., Waite, J. H., Paranicas, C. P., & Williams, D. J. (2002). Transient aurora on Jupiter from injections of magnetospheric electrons. *Nature*, *415*(6875), 1003–1005. https://doi.org/10.1038/4151003a

Mauk, B. H., Haggerty, D. K., Jaskulek, S. E., Schlemm, C. E., Brown, L. E., Cooper, S. A., et al. (2017). The Jupiter energetic particle detector instrument (JEDI) Investigation for the Juno mission. *Space Science Reviews*, *213*(1), 289–346. https://doi.org/10.1007/s11214-013-0025-3

Mauk, B. H., Williams, D. J., McEntire, R. W., Khurana, K. K., & Roederer, J. G. (1999). Storm-like dynamics of Jupiter's inner and middle magnetosphere. *Journal of Geophysical Research*, *104*(A10), 22759–22778. https://doi.org/10.1029/1999JA900097

McComas, D. J., Alexander, N., Allegrini, F., Bagenal, F., Beebe, C., Clark, G., et al. (2017). The Jovian auroral distributions experiment (JADE) on the Juno mission to Jupiter. *Space Science Reviews*, *213*(1), 547–643. https://doi.org/10.1007/s11214-013-9990-9

Morgenthaler, J. P., Rathbun, J. A., Schmidt, C. A., Baumgardner, J., & Schneider, N. M. (2019). Large volcanic event on Io Inferred from Jovian sodium nebula brightening. *The Astrophysical Journal Letters*, *871*(2), L23. https://doi.org/10.3847/2041-8213/aafdb7

Nichols, J. D. (2023). Jupiter's FUV auroras during the Juno EM [Dataset]. Mikulski Archive for Space Telescopes. https://doi.org/10.17909/zdfp-m905

Nichols, J. D., Allegrini, F., Bagenal, F., Bunce, E. J., Cowley, S. W. H., Ebert, R. W., et al. (2020). An enhancement of Jupiter's main auroral emission and magnetospheric currents. *Journal of Geophysical Research: Space Physics*, *125*(8), e2020JA027904. https://doi.org/10.1029/2020JA027904

Nichols, J. D., Badman, S. V., Bagenal, F., Bolton, S. J., Bonfond, B., Bunce, E. J., et al. (2017). Response of Jupiter's auroras to conditions in the interplanetary medium as measured by the Hubble Space Telescope and Juno. *Geophysical Research Letters*, *44*(15), 7643–7652. https://doi.org/10.1002/2017GL073029

Nichols, J. D., Badman, S. V., Baines, K. H., Brown, R. H., Bunce, E. J., Clarke, J. T., et al. (2014). Dynamic auroral storms on Saturn as observed by the Hubble Space Telescope. *Geophysical Research Letters*, *41*(10), 3323–3330. https://doi.org/10.1002/2014gl060186

Nichols, J. D., Clarke, J. T., Gérard, J.-C., Grodent, D., & Hansen, K. C. (2009). Variation of different components of Jupiter's auroral emission. *Journal of Geophysical Research*, *114*(A6), A06210. https://doi.org/10.1029/2009ja014051

Nichols, J. D., & Cowley, S. W. H. (2022). Relation of Jupiter's dawnside main emission intensity to magnetospheric currents during the Juno Mission. *Journal of Geophysical Research: Space Physics*, *127*(1), e2021JA030040. https://doi.org/10.1029/2021JA030040

Nichols, J. D., Yeoman, T. K., Bunce, E. J., Chowdhury, M. N., Cowley, S. W. H., & Robinson, T. R. (2017). Periodic emission within Jupiter's main auroral oval. *Geophysical Research Letters*, *44*(18), 9192–9198. https://doi.org/10.1002/2017GL074824

Swithenbank-Harris, B., Nichols, J., Allegrini, F., Bagenal, F., Bonfond, B., Bunce, E., et al. (2021). Simultaneous observation of an auroral dawn storm with the Hubble Space Telescope and Juno. *Journal of Geophysical Research: Space Physics*, *126*(4), e2020JA028717. https://doi.org/10.1029/2020ja028717

Waite, J. H., Cravens, T. E., Kozyra, J., Nagy, A. F., Atreya, S. K., & Chen, R. H. (1983). Electron precipitation and related aeronomy of the Jovian thermosphere and ionosphere. *Journal of Geophysical Research*, *88*(A8), 6143–6163. https://doi.org/10.1029/JA088iA08p06143

Yao, Z. H., Bonfond, B., Clark, G., Grodent, D., Dunn, W. R., Vogt, M. F., et al. (2020). Reconnection- and dipolarization-driven auroral dawn storms and injections. *Journal of Geophysical Research: Space Physics*, *125*(8), e2019JA027663. https://doi.org/10.1029/2019JA027663

References From the Supporting Information

Cowley, S., Nichols, J., & Bunce, E. (2002). Distributions of current and auroral precipitation in Jupiter's middle magnetosphere computed from steady-state Hill-Pontius angular velocity profiles: Solutions for current sheet and dipole magnetic field models. *Planetary and Space Science*, *50*(7–8), 717–734. https://doi.org/10.1016/s0032-0633(02)00046-6

Guio, P., Staniland, N. R., Achilleos, N., & Arridge, C. S. (2020). Trapped particle motion in magnetodisk fields. *Journal of Geophysical Research: Space Physics*, *125*(7), e2020JA027827. https://doi.org/10.1029/2020JA027827

Hamlin, D. A., Karplus, R., Vik, R. C., & Watson, K. M. (1961). Mirror and azimuthal drift frequencies for geomagnetically trapped particles. *Journal of Geophysical Research*, *66*(1), 1–4. https://doi.org/10.1029/JZ066i001p00001

Khurana, K. K. (1997). Euler potential models of Jupiter's magnetospheric field. *Journal of Geophysical Research*, *102*(A6), 11295–11306. https://doi.org/10.1029/97JA00563

Lew, J. S. (1961). Drift rate in a dipole field. *Journal of Geophysical Research*, *66*(9), 2681–2685. https://doi.org/10.1029/JZ066i009p02681

Mauk, B. H., Williams, D. J., & McEntire, R. W. (1997). Energy-time dispersed charged particle signatures of dynamic injections in Jupiter's inner magnetosphere. *Geophysical Research Letters*, *24*(23), 2949–2952. https://doi.org/10.1029/97GL03026